# Expanded View Figures

**Figure EV1. MOAP-1 is a negative regulator of p62 bodies.**

A MOAP-1 downregulates the levels of the MG132-induced p62 bodies in a time-dependent manner. HepG2 cells stably expressing GFP-MOAP-1 or GFP were treated with MG132 (5 μM) for the indicated durations before being subjected to IF analysis with anti-GFP (in green) and anti-p62 (in red) antibodies.

B MOAP-1 regulates levels of p62 bodies in HeLa cervical cancer cells. WT and *MOAP-1* KO HeLa cells were subjected to IF analysis with the anti-p62 antibody (in red).

C Quantification of the p62 bodies in the WT and *MOAP-1* KO HeLa cells. (Left panel) number of p62 bodies per cell. $n = 7$ independently plated samples. (Right panel) size of p62 bodies. $n = 164$ and 410 bodies detected in the WT and *MOAP-1* KO cells, respectively, from three independently plated samples.

D Deficiency in MOAP-1 does not alter total protein levels of p62 in the HeLa cells. Western blotting analysis of p62 protein levels in the WT and *MOAP-1* KO HeLa cells.

E Effect on the reduction of p62 bodies during the washout period after arsenic trioxide treatment is weaker in the *MOAP-1* KO MEFs. WT and *MOAP-1* KO MEFs were treated with arsenic trioxide ($As_2O_3$, 10 μM) for 12 h. The cells were washed three times. At 6 or 12 h post-washing, the cells were harvested for IF analysis with anti-p62 antibody (in red).

F Quantification of the p62 bodies in the WT and *MOAP-1* KO MEFs treated with $As_2O_3$ and at the indicated times during the washout period. (Upper panel) number of p62 bodies per cell. $n = 6$ independently plated samples. (Lower panel) size of p62 bodies. $n = 318$ (WT, basal), 273 (*MOAP-1* KO, basal), 532 (WT, $As_2O_3$ 12 h),1207 (*MOAP-1* KO, $As_2O_3$ 12 h), 164 (WT, washout 6 h), 571 (*MOAP-1* KO, washout 6 h), 139 (WT, washout 12 h) and 725 bodies (*MOAP-1* KO, washout 12 h) from three independently plated samples.

G MOAP-1 deficiency does not overtly alter the protein levels of p62 in the MEFs upon washout of $As_2O_3$. Western blotting analysis of p62 and MOAP-1 in the WT and *MOAP-1* KO MEFs treated with $As_2O_3$ and at the indicated times during the washout period. MOAP-1 was immunoprecipitated from the lysates. Actin as loading control.

H MOAP-1 deficiency elevates levels of p62 protein in the detergent-insoluble fractions in LO2 and HeLa cells. LO2 and HeLa cells with the indicated genotypes were lysed in 1% Triton X lysis buffer, separated into detergent-soluble (S) and insoluble (I) fractions and analyzed by Western blotting. *p62* KO LO2 cells were included as a negative control to validate the specificity of the p62 protein band detected in these fractions. Coomassie Brilliant Blue (CBB)-stained gels were included to show comparable loading of the insoluble fractions in the samples.

Data information: In (A, B, E) Nuclei were counterstained with DAPI (blue). Scale bar: 10 μm. In (C, F), error bars represent SEM. $*P < 0.05$, $**P < 0.01$, $***P < 0.001$, ns, not significant, Student's *t*-test.

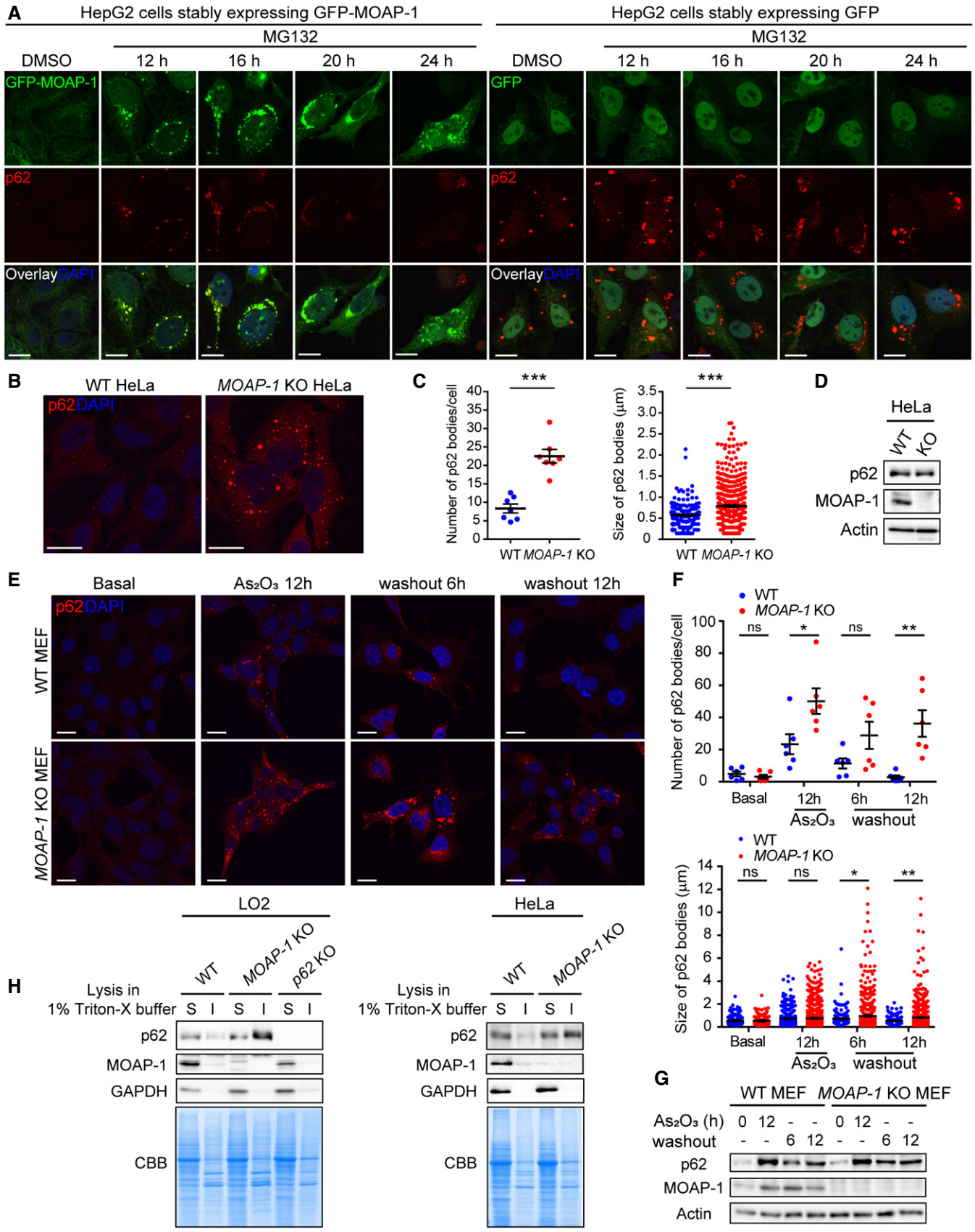


**Figure EV1.**

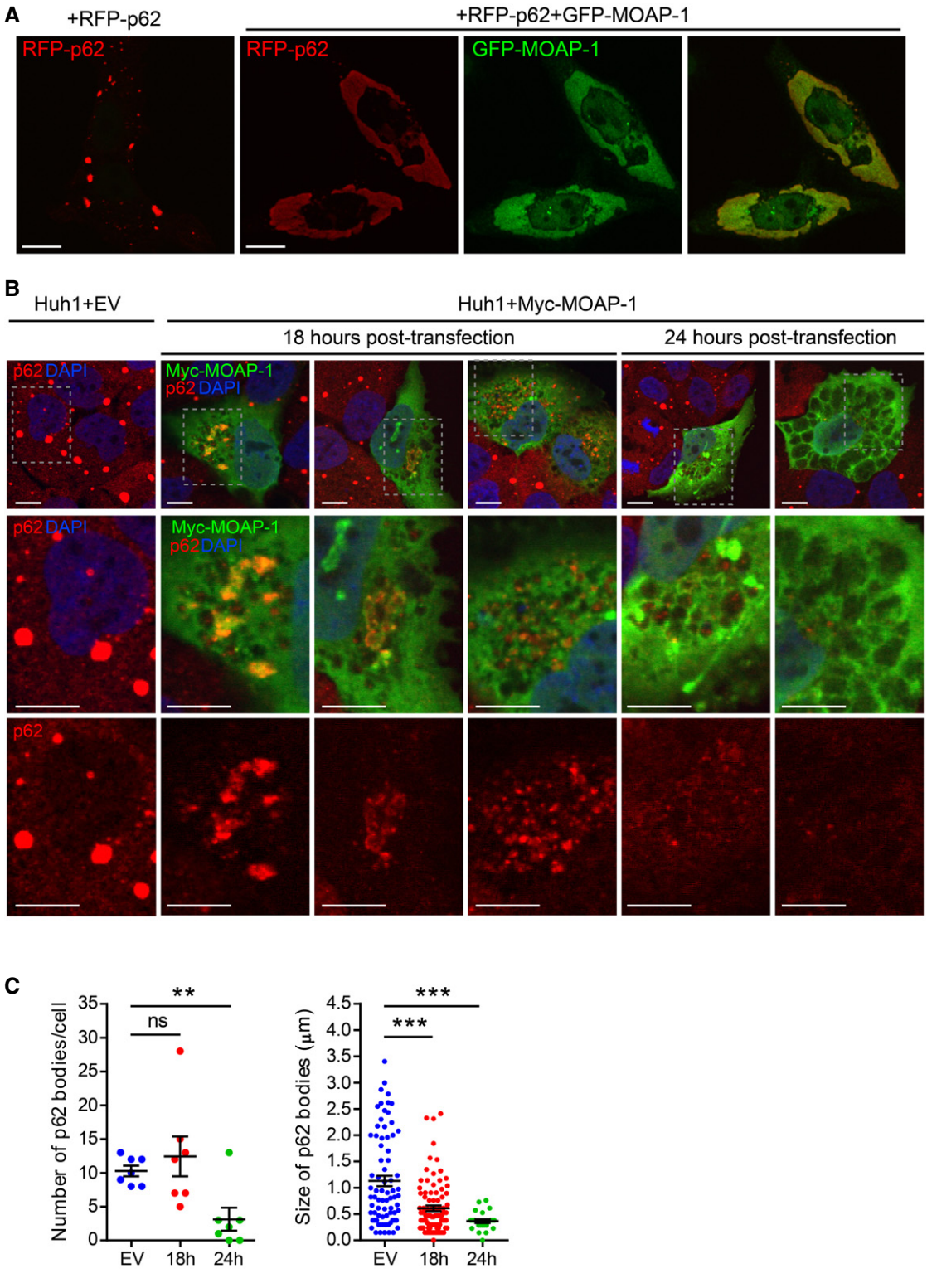


**Figure EV2.**

**Figure EV2. Overexpression of MOAP-1 disrupts the spherical structure of p62 bodies.**

A Liquid phase condensation of p62 is impaired in the cells overexpressing MOAP-1. LO2 cells were transfected with expression vectors encoding RFP-p62 with or without GFP-MOAP-1 for 24 h. Scale bar: 5 μm.

B Huh1 cells were transfected with expression vector encoding Myc-MOAP-1 or empty vector (EV), and harvested at 18- or 24-h post-transfection for IF analysis using anti-p62 (in red) and anti-Myc (in green) antibodies. Insets were enlarged in the lower panels. Nuclei were stained with DAPI (in blue). Scale bar: 5 μm.

C Quantification of the p62 bodies in the Huh1 cells transfected with empty vector (EV) or Myc-MOAP-1 for 18 or 24 h as described in (B). (Left panel) number of p62 bodies per cell. $n = 7$ independently plated samples. (Right panel) size of p62 bodies. $n = 77$, 91, and 22 bodies detected in the EV, Myc-MOAP-1 transfected cells at 18- and 24-h post-transfection, respectively, from three independently plated samples. Error bars represent SEM. $^{**}P < 0.01$, $^{***}P < 0.001$, ns, not significant, Student's *t*-test.

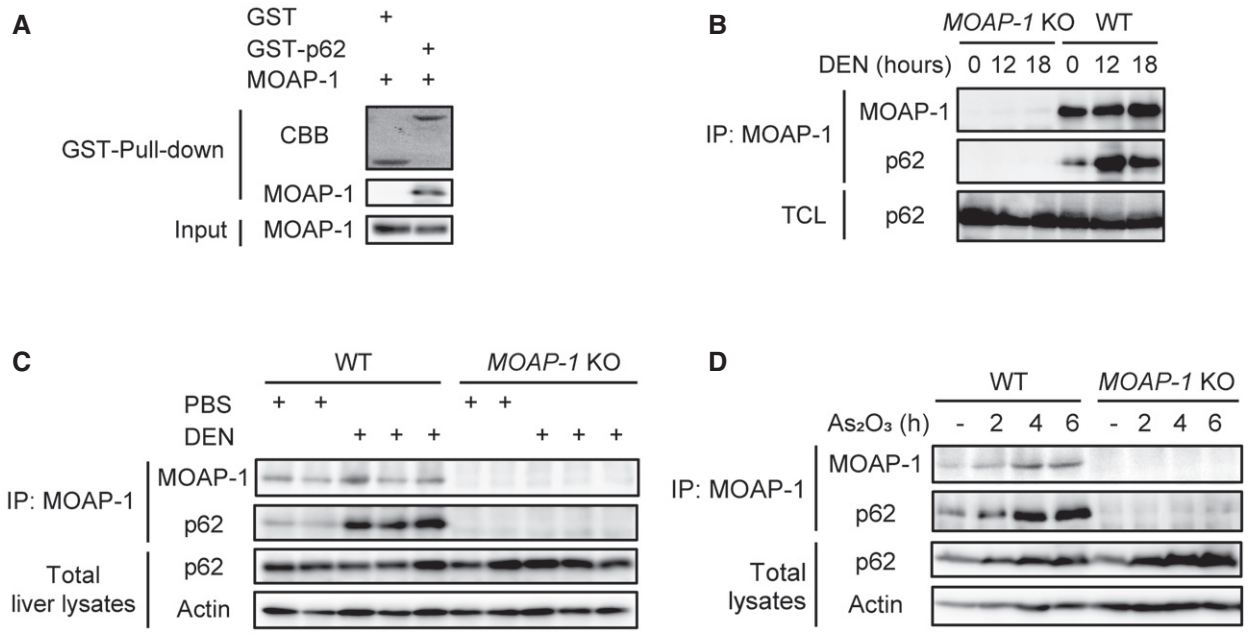


**Figure EV3. MOAP-1 interacts with p62 and the interaction is enhanced by treatment with DEN or arsenic trioxide.**

A MOAP-1 binds p62 *in vitro*. Recombinant proteins of MOAP-1 and GST-p62 or GST control (1μg each) were incubated for 2 h and the mixture was subjected to GST pull-down. Eluates from the pull-down and input (1% of the pre-pull-down mixtures) were analyzed by Western blotting or SDS–PAGE followed by Coomassie Brilliant Blue (CBB) staining to detect GST and GST-p62 proteins in the pull-down.

B, C Co-IP assay performed on the LO2 cells treated with or without diethylnitrosamine (DEN, 200 μM) for the indicated times (B) or liver lysates prepared from wild-type mice injected with PBS or DEN (100 μg/g body weight) for 48 h (C). TCL, total cell lysates.

D Co-IP assay performed on the MEFs treated with $As_2O_3$ (10 μM) for the indicated period of times.

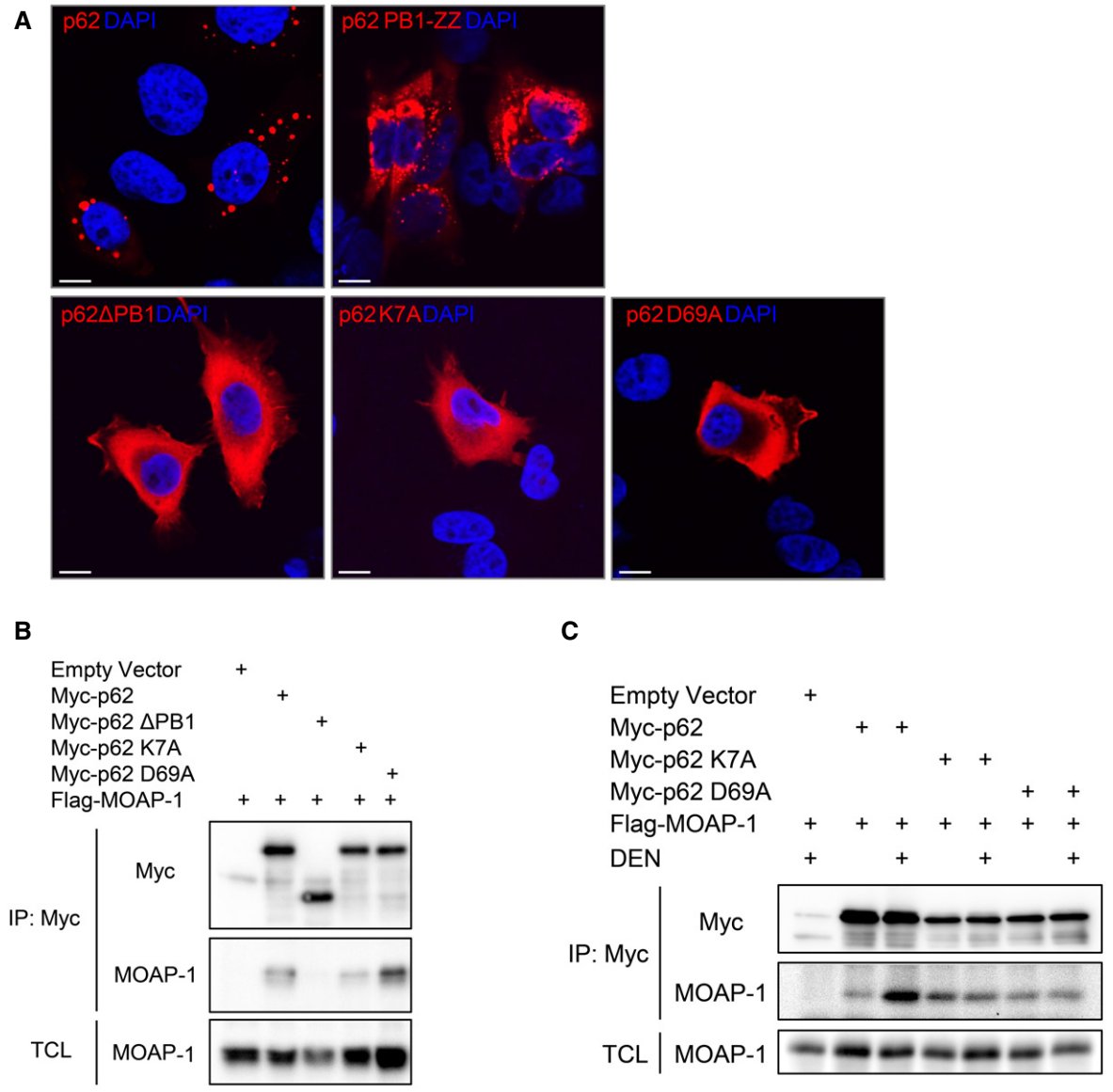


**Figure EV4. Oligomerization of p62 is a pre-requisite for its enhanced interaction with MOAP-1 under DEN conditions.**

A The fragment of p62 encompassing the PB1 and ZZ domains is not fully competent in forming aggregates compared to the full-length p62, while the mutant of p62 lacking the PB1 domain and the K7A and D69A mutants all fail to form aggregates. *p62* KO LO2 hepatocytes were transfected with Myc-p62 or the indicated mutants for 24 h and subjected to immunofluorescence using anti-Myc antibody (in red). Nuclei were stained with DAPI (in blue). Scale bar: 10 μm.

B The K7A and D69A mutants of p62, which fail to oligomerize, retained their ability to interact with MOAP-1. *p62* KO LO2 hepatocytes were transfected with Myc-p62 or the indicated mutants and Flag-MOAP-1 for 24 h and subjected to co-IP assay using anti-Myc antibody. TCL, total cell lysates.

C DEN treatment enhances interaction between MOAP-1 and p62, but not the K7A and D69A mutants. *p62* KO LO2 hepatocytes were transfected with Myc-p62 or the indicated mutants and Flag-MOAP-1 for 24 h and treated with diethylnitrosamine (DEN, 200 μM) for 12 h before being subjected to co-IP assay using anti-Myc antibody.

 

**Figure EV5. Loss of MOAP-1 promotes p62-dependent activation of Nrf2.**

A Increased recruitment of Keap1 to the p62 bodies in the *MOAP-1* KO HeLa cells. WT and *MOAP-1* KO HeLa cells were subjected to IF analysis with anti-Keap1 (green) and anti-p62 (red) antibodies. Insets in the upper panels are enlarged in the lower panels. Nuclei were counterstained with DAPI (in blue). Scale bar: 5 μm.

B MOAP-1 deficiency promotes activation of Nrf2 signaling in HeLa cells. Transcript levels of downstream targets of Nrf2 (*HMOX-1*, *NQO1*, *SLC7A11*, *GCLC*, and *G6PD*) in WT and *MOAP-1* KO HeLa cells were determined by RT–PCR and normalized to GAPDH.

C Increased levels of HMOX1 in *MOAP-1* KO MEFs upon treatment with arsenic trioxide. WT and *MOAP-1* KO MEFs were treated with $As_2O_3$ (10 μM) for the indicated hours and cells were harvested for Western blotting.

D Elevated transcriptional activity of Nrf2 in the MOAP-1-deficient cells is mediated through p62. WT, *MOAP-1* KO, and *MOAP-1/p62* double KO (DKO) LO2 cells were transfected with antioxidant response element (ARE)-firefly luciferase and renilla luciferase reporter constructs for overnight and subjected to dual luciferase assay. Normalized firefly to renilla luciferase activities in relative to that of untreated WT were plotted.

E Re-expression of MOAP-1, but not the p62-binding-defective MOAP-1-M3 mutant, reduces the recruitment of Keap1 to p62 bodies in the MOAP-1-deficient LO2 cells. *MOAP-1* KO LO2 cells stably expressing GFP-MOAP-1 or GFP-MOAP-1-M3 were subjected to IF analysis with anti-Keap1 (green) and anti-p62 (red) antibodies. Insets in the upper panels are enlarged in the lower panels. Nuclei were counterstained with DAPI (in blue). Scale bar: 5 μm.

F Re-expression of MOAP-1, but not the MOAP-1-M3 mutant, restores the Keap1/Nrf2 interaction in the *MOAP-1* KO LO2 cells. *MOAP-1* KO LO2 cells stably expressing GFP-MOAP-1 or GFP-MOAP-1-M3 were subjected to Duolink proximity ligation assay using anti-Keap1 and anti-Nrf2 antibodies. Red dots represent Keap1/Nrf2 interaction. Nuclei were counterstained with DAPI (in blue). Scale bar: 10 μm.

G Quantification of the Duolink signals as described in (F). Duolink signals were quantified by ImageJ analysis and normalized to the number of nuclei.

H Re-introduction of MOAP-1, but not the MOAP-1-M3 mutant, reduces nuclear levels of Nrf2 in the *MOAP-1* KO LO2 cells. *MOAP-1* KO LO2 cells stably expressing GFP-MOAP-1 or GFP-MOAP-1-M3 were subjected to IF analysis with the anti-Nrf2 antibody. Scale bar: 10 μm.

I Quantification of nuclear levels of Nrf2 as described in (H). The mean gray values of Nrf2 fluorescence signals were quantified by ImageJ analysis.

J MOAP-1, but not the M3 mutant, reduces the transcriptional activity of Nrf2 target genes. Transcript levels of downstream targets of Nrf2 (*HMOX-1*, *NQO1*, *SLC7A11*, *GCLC*, and *G6PD*) in the *MOAP-1* KO LO2 cells stably expressing GFP-MOAP-1 or GFP-MOAP-1-M3 were determined by RT–PCR and normalized to GAPDH.

K Western blotting of *MOAP-1* KO LO2 cells stably expressing GFP-MOAP-1 or GFP-MOAP-1-M3 mutant as described in (E-J).

Data information: In (B, D, G, I, J), error bar represents SEM. $*P < 0.05$, $**P < 0.01$, $***P < 0.001$, ns, not significant, Student's *t*-test. Averages of three independent experiments were plotted.

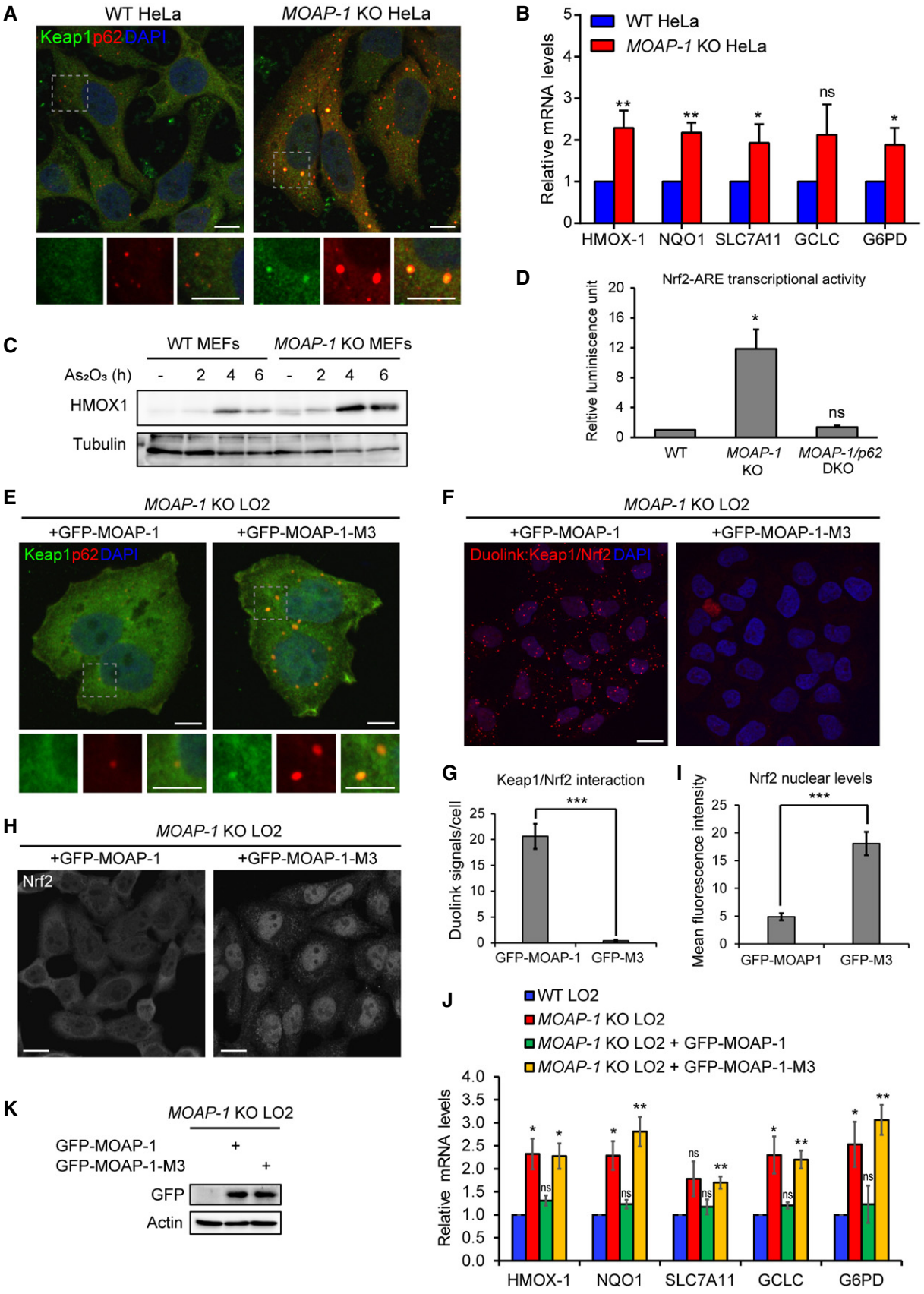


**Figure EV5.**